[CANCER RESEARCH 64, 2167–2174, March 15, 2004]

Epstein-Barr Virus Infection of Human Natural Killer Cell Lines and Peripheral Blood Natural Killer Cells

Yasushi Isobe,[1] Koichi Sugimoto,[1] Lixin Yang,[2] Kenji Tamayose,[1] Motoki Egashira,[1] Takako Kaneko,[1] Kenzo Takada,[2] and Kazuo Oshimi[1]

[1]Division of Hematology, Department of Medicine, Juntendo University School of Medicine, Bunkyo-ku, Tokyo, and [2]Department of Tumor Virology, Institute for Genetic Medicine, Hokkaido University, Sapporo, Japan

ABSTRACT

Although considerable part of natural killer (NK) cell neoplasms possess EBV genome, there has been no direct evidence that EBV infects human NK cells *in vitro*. In this study, we demonstrated EBV entry into NK cells using a recombinant EBV, which contains enhanced green fluorescent protein (EGFP) gene in its genome (EGFP-EBV). After 48 h of exposure to EGFP-EBV, we detected EGFP signals in ~30% of NK-92 and NKL cells and >40% of peripheral blood NK cells from three healthy volunteers. Reverse transcription-PCR analysis of various EBV-associated genes confirmed EBV infection. *In situ* hybridization for *EBERs* and *BHLFs* showed that latent and lytic infections coexisted at the early phase of EBV infection in two NK cell lines. Although *BHLF*-positive cells in the early lytic phase were round-shaped, *EBER*-positive cells in latent EBV infection tended to show a bizarre shape. Flow cytometric analysis of EGFP-EBV-exposed NK cell lines showed that most of EBV-infected cells entered early apoptosis after 72 h of EBV exposure, which explains the difficulties to establish EBV-carrying NK clones. Flow cytometry and reverse transcription-PCR analysis indicated that two NK cell lines may fuse with EBV using HLA class II after binding to the virus through a distinct molecule from CD21. We established two EBV-carrying NKL clones showing latency types I and II, both of which are recognized in EBV-associated NK cell neoplasms. Because EBV-infected NKL cells showed only type I latency during the early phase of infection, the temporal profile of latent gene expression is similar to that of T cells. We first report *in vitro* EBV infection of human NK cells and establishment of EBV-carrying NK clones, which should contribute to elucidate the role of EBV in the development of NK cell neoplasms.

INTRODUCTION

EBV is a human herpesvirus carried by the majority of human population. Primary EBV infection causes infectious mononucleosis. Persistent EBV infection is associated with various lymphoid and epithelial malignancies, including Burkitt lymphoma, Hodgkin lymphoma, peripheral T-cell lymphoma, and nasopharyngeal carcinoma (1, 2). Recent reports suggest that the EBV infection is closely associated with mature natural killer (NK) cell malignancies (3–6).

Lymphoproliferative disorders of mature NK cells consist of nasal-type NK cell lymphoma, aggressive NK cell leukemia/lymphoma, and chronic NK lymphocytosis (7–11). Nasal-type NK cell lymphoma frequently arises in eastern Asia and Central and South America. Some cases of lethal midline granuloma correspond to nasal-type NK cell lymphoma. Necrosis and angiodestructive infiltration of tumor cells are histological features of the disease (6, 7). The patients present coagulopathy and multiorgan failure at the advanced stage, and the prognosis is very poor (8). Aggressive NK cell leukemia/lymphoma is a fatal disease, which is characterized by high fever, lymphadenopathy, hepatosplenomegaly, and atypical granular lymphocytes proliferation in the peripheral blood (7, 9). In contrast, most cases of chronic NK lymphocytosis are asymptomatic and require no treatment (10, 11).

EBV entry into target cells usually results in lytic or latent infection (2, 12). In the lytic infection, the viral structural genes are all transcribed, which leads to virion production and the resultant cell lysis of host cells. The latent infection is predominantly nonproductive and characterized by expression of six EBV-determined nuclear antigens genes (*EBNA1*, *EBNA2*, *EBNA3A*, *EBNA3B*, *EBNA3C*, and *EBNA-LP*), three latent membrane proteins genes (*LMP1*, *2A*, and *2B*), *Bam*HI A rightward transcripts, and two abundant EBV-encoded nonpolyadenylated RNAs (*EBER1* and *EBER2*; Refs. 2, 12). Lymphoblastoid cell lines transformed by EBV *in vitro* demonstrate the full pattern of gene expression, which is defined as type III latency. In contrast, the latent gene expression is more restricted in EBV-associated malignancies (1, 2). Burkitt lymphoma expresses *EBERs*, *EBNA1*, and *Bam*HI A rightward transcripts, which corresponds to type I latency. In Hodgkin lymphoma, peripheral T-cell lymphoma, and nasopharyngeal carcinoma, a range of the latent gene expression is extended to *LMPs*. The pattern corresponds to type II latency. In EBV-associated NK cell malignancies, there have shown that the gene expression pattern corresponds to type I or II latency (13, 14).

Many studies have shown that the neoplastic NK cells possess monoclonal EBV genome, which indicates that latent EBV infection occurs before the clonal expansion (3–5). In almost all of the cases of nasal-type NK cell lymphomas, tumor cells contain EBV (6, 7). This suggests that EBV should play an important role in the pathogenesis of the disease. EBV is also frequently detectable in the Japanese cases of aggressive NK cell leukemia/lymphoma (11, 14). Chronic NK lymphocytosis with hypersensitivity to mosquito bites is known as a distinct entity related to chronic active EBV infection (15). The proliferating NK cells are infected with EBV. Such cases occasionally take a progressive course and consequently lead to aggressive NK cell leukemia/lymphoma (15, 16). However, the manner of EBV infection has never been elucidated in human NK cells.

EBV entry into B cells requires multiple interactions between viral and cellular molecules. Binding of the major viral capsid glycoprotein, gp350/220, to CD21 mediates the initial EBV attachment to B cells (17, 18). Viral internalization into B cells depends on an additional interaction between gp85-gp25-gp42 viral glycoprotein complex and HLA class II molecules (18–21). Recent studies, however, suggest that CD21-independent mechanism may exist for EBV infection, especially in epithelial cells (21–25).

In this study, we detected the EBV entry into human NK cells and cell lines using the recombinant EBV (rEBV) that contains enhanced green fluorescent protein (EGFP) gene in its genome (25, 26). This method clearly shows EBV infection even before the establishment of persistent infection.

MATERIALS AND METHODS

Virus. In this study, we used two types of rEBV: neo^r-EBV and EGFP-EBV. In neo^r-EBV, the neomycin resistance gene (*NEO^r*) is inserted at the site of *BXLF1*, which encodes EBV thymidine kinase. EGFP-EBV contains

Received 6/6/03; revised 10/20/03; accepted 12/31/03

The costs of publication of this article were defrayed in part by the payment of page charges. This article must therefore be hereby marked *advertisement* in accordance with 18 U.S.C. Section 1734 solely to indicate this fact.

Requests for reprints: Koichi Sugimoto, Division of Hematology, Department of Medicine, Juntendo University School of Medicine, 2-1-1 Hongo, Bunkyo-ku, Tokyo 113-8421, Japan.

NEO^r plus reporter EGFP gene at the same site to visualize EBV infection in living cells. Details of rEBV generation are described previously (25, 27).

Cell Lines. As the target cells, we used NK-92 and NKL, which were derived from leukemic cells of each aggressive NK cell leukemia/lymphoma patient (28, 29). Both NK cell lines are grown in Iscove's modified Dulbecco's medium (Invitrogen, Grand Island, NY) supplemented with 10% heat-inactivated fetal bovine serum (Intergen, Purchase, NY), 2 mM glutamine (Invitrogen), 100 units/ml penicillin (Invitrogen), 100 μg/ml streptomycin (Invitrogen). Human interleukin-2 is essential for maintenance of both NK cell lines (100 units/ml, provided by Shionogi, Osaka, Japan). Akata, a Burkitt lymphoma-derived cell line, infected with neo^r-EBV or EGFP-EBV, was used as rEBV-producing cells (30, 31). Akata was maintained in RPMI 1640 (Sigma, St. Louis, MO) with the same supplements and 700 μg/ml G418 (Invitrogen). Raji (EBV-positive, CD21-positive) and U937 (EBV-negative, CD21-negative) were used as positive and negative controls, respectively. They were supplied from Japanese Cancer Research Resources Bank.

Purification of Peripheral Blood NK (PB-NK) Cells. PB-NK cells were isolated from heparinized venous blood obtained from three healthy volunteers. NK cell-rich mononuclear cells were isolated by centrifugation in Ficoll-Hypaque gradient using RosetteSep NK cell cocktail (StemCell Technologies, Vancouver, British Columbia, Canada). PB-NK cells were purified by negative depletion with OKT3 (anti-CD3; Ortho Diagnostic Systems, Raritan, NJ), BL1a (anti-CD5; Coulter, Miami, FL), and B1 (anti-CD20; Coulter) monoclonal antibodies (mAbs). Positively labeled cells were removed with Dynabeads goat anti-pan mouse IgG (Dynal, Oslo, Norway). Trypan blue-dye exclusion procedure showed that >99% of the purified cells were viable. Evaluation by CYTRON ABSOLUTE flow cytometer (Ortho Diagnostic Systems) confirmed that the preparation contained >98% of NK cells ($CD3^-$ $CD16^+$ or $CD3^-CD56^+$ cells).

Virus Production and Infection Procedure. We obtained infectious rEBV from Akata cells by surface immunoglobulin cross-linking as described previously (31). Each rEBV concentrate was resuspended into 1.5×10^7 particles/μl. The concentrate (250 μl) was added to 250 μl of the cell suspension (2.5×10^6 cells) in a polypropylene tube. Cells were incubated with rEBV for 2 h at 37°C and resuspended (2×10^5/ml) in culture medium and incubated. After 48 h of incubation, the cells were harvested and analyzed. The other cells were reseeded into 96-well plates at 10^2/well in culture medium containing 700 μg/ml G418 (Invitrogen).

Reverse Transcription-PCR (RT-PCR) Analysis. Briefly, cDNA synthesis was performed from 800 ng of total RNA and 100 pmol of random hexamer (Takara, Otsu, Japan) using Superscript II reverse transcriptase (Invitrogen) in a volume of 20 μl. For PCR amplification, 1 μl of cDNA was added to 49 μl of PCR reaction mixture containing 1.25 units of TaqDNA polymerase (Takara). To analyze EBV-associated gene transcripts, we performed nested PCR analysis. Details of the sequences of primers and PCR conditions are given in Table 1.

Propidium Iodide (PI) Rejection and Annexin V Binding Assays. We evaluated cell death process of rEBV-exposed NK cell lines by PI and annexin V binding assays using Annexin V-Biotin Kit (Coulter). Each cell suspension (4×10^6/ml) of both NK cell lines was exposed to EGFP-EBV as described above. The cells were collected and washed with $CaCl_2$-containing binding buffer (Coulter). Each cell suspension (2×10^4/ml) was mixed with 2.5 μg/ml PI or biotinylated annexin V (Coulter) for 10 min at 4°C. Cells mixed with PI were subsequently washed, fixed with 2% paraformaldehyde/PBS for 20 min at room temperature, and analyzed. Cells mixed with biotinylated annexin V were washed, resuspended in 100 μl of binding buffer, and incubated with ECD-labeled streptavidin for 30 min at room temperature. They were washed, fixed with 2% paraformaldehyde/PBS, and analyzed by flow cytometry.

Detection of EGFP by Fluorescence Microscopy and Flow Cytometry. rEBV-exposed and control cells were collected, washed once, and resuspended at the concentration of 5×10^5/ml in 35-mm Glass Bottom Microwell Dishes (Mat Tek, Ashland, MA). The green fluorescence was analyzed using Zeiss LSM510 confocal laser scanning microscope (Carl Zeiss, Jena, Germany). Part of these cells were directly fixed with 0.4% paraformaldehyde/PBS and analyzed by flow cytometry.

RNA *in Situ* Hybridization. Cells were collected, washed twice with 1× PBS, and concentrated. Cell preparations on slide glasses were fixed with 4% paraformaldehyde/PBS at room temperature for 20 min. After treating them with proteinase K (DAKO, Glastrup, Denmark), we used FITC-labeled peptide nucleic acid probes for *EBERs* (*EBER1* and *EBER2*) and *Bam*HI H fragments, lower strand frames (*BHLFs*) (*BHLF1* and *BHLF2*; DAKO), and evaluate the expression using PNA ISH Detection kit (DAKO) according to the manufacture's instructions.

Cell Surface and Intracytoplasmic Expression Analysis by Flow Cytometry. One $\times 10^5$ cells were labeled with various mouse mAbs described below, followed by the addition of phycoerythrin-conjugated goat antimouse mAb (Coulter). Fcγ receptors on the cell surfaces were blocked

Table 1 *Oligonucleotides used for reverse transcription-PCR analysis*

Transcripts	Primer	Product size	Sequences (5′–3′)	Coordinates in B95-8	Annealing temperature, PCR cycle	Reference
Qp-initiated	Q external	330	AGGCGCGGGATAGCGTGCGCTACCGGA	62426–62452	1st: 45°C, 35 cycles	32
EBBA1	Q internal		ATAGCGTGCGCTACCGGATGG	62435–62455		Original
	K external		CACCATCTCTATGTCTTGGC	108157–108138	2nd: 45°C, 35 cycles	Original
	K internal		TCCTCGTCCATGGTTATCAC	108075–108056		32
EBNA2	W2-Y1	339	GGTTCACCTTCAGGGCCACT	45538–45552, 47761–47765	1st: 55°C, 35 cycles	Original
	Y2		GCTGCTACGCATTAGAGACC	47892–47911		32
	3′ external		ACCCCCGTGTTTTCCCCAAC	48676–48657	2nd: 70°C, 35 cycles	Original
	3′ internal		TCCTGGTAGGGATTCGAGGG	48616–48597		32
LMP1	5′ external	324	TCCTCCTCTTGGCGCTACTG	169383–169364	1st: 45°C, 35 cycles	32
	5′ internal		CCTACTGATGATCACCCTCCT	169217–169207, 169128–169119		Original
	3′ external		GGAGTCATCGTGGTGGTGTT	168721–168740	2nd: 68°C, 35 cycles	Original
	3′ internal		TCATCACTGTGTCGTTGTCC	168740–168759		32
LMP2A	5′ external	280	GCAACACGACGGGAATGACG	166824–166843	1st: 45°C, 35 cycles	33
	5′ internal		ATGACTCATCTCAACACACATA	166874–166893		34
	3′ external		CTGCGGCCAGCAATGCAAAC	434–415	2nd: 68°C, 35 cycles	Original
	3′ internal		CATGTTAGGCAAATTGCAAA	381–362		34
BZLF1	5′ external	318	CTCCTTTGCCTTGTGTGCTGT	103031–103011	1st: 55°C, 35 cycles	Original
	5′ internal		CATGTTTCAACCGCTCCGACTGG	102963–102941		32
	3′ external		GCGCAGCCTGTCATTTTCAGATG	102303–102325	2nd: 68°C, 35 cycles	32
	3′ internal		TTCCTCCAGCGATTCTGGCT	102665–102655, 102530–102522		Original
BALF2	5′ external	118	GTCAAGATGTTCAAGGACGTGG	163094–163072	1st: 55°C, 35 cycles	35
	5′ internal		GGTCAAGAGCTGCTACCACG	162998–162978		35
	3′ external		CTCATAGCACATACAGATGGGC	162856–162878	2nd: 68°C, 35 cycles	35
	3′ internal		GGAGATGTCCTGCAGGATGG	162881–162901		35
EBER1	5′	167	AGGACCTACGCTGCCCTAGA	6629–6648	55°C, 35 cycles	34
	3′		AAAACATGCGGACCACCAGC	6795–6776		34
CD21	SCR2-5′	327	GTTGTTCAGGTACCTTCCGC		62°C, 35 cycles	23, 41
	SCR3-3′		TAGGAAGTGCTGGACACTCG			23, 41
β-actin	CytA-5′	202	CCTTCCTGGGCATGGAGTCCT		62°C, 35 cycles	36
	CytA-3′		GGAGCAATGATCTTGATCTTC			36

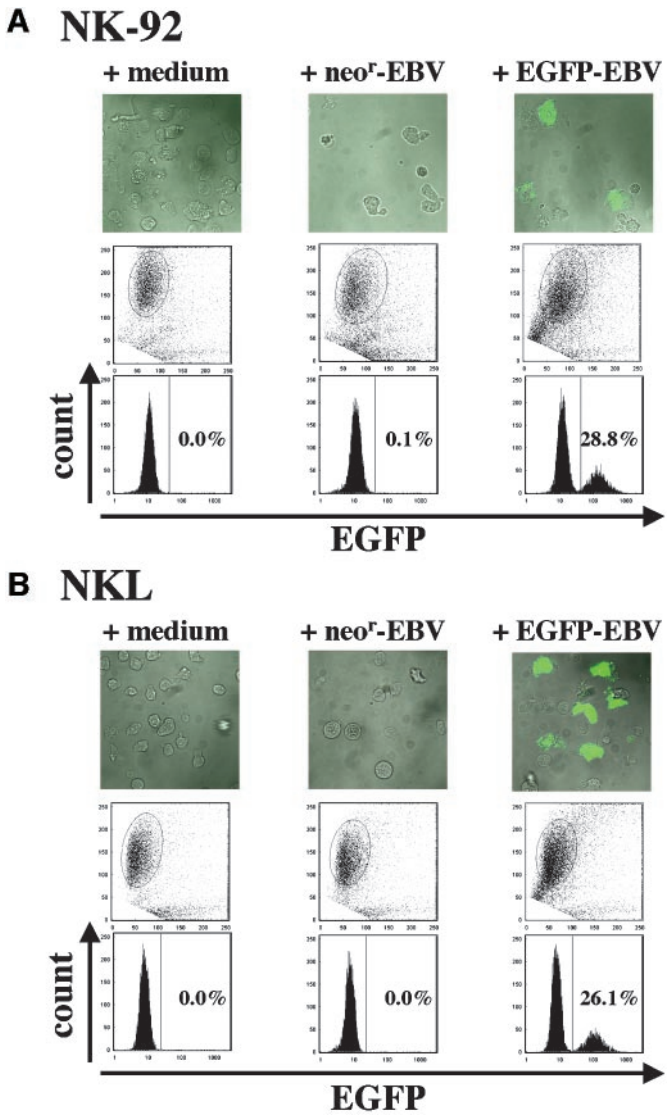

Fig. 1. Enhanced green fluorescent protein (EGFP) expression in NK-92 and NKL cells infected by EGFP-EBV. NK-92 (*A*) and NKL (*B*) were incubated for an additional 46 h after 2 h of exposure to medium, neo^r-EBV or EGFP-EBV. Confocal laser microscopy (*top column*) and flow cytometry (*middle and bottom columns*) detected EGFP signal only in EGFP-EBV-exposed NK-92 and NKL cells.

with human immunoglobulin (provided by Mitsubishi Pharma, Osaka, Japan). The labeled cells were analyzed by flow cytometry. We used OKB7 (IgG2a; Ortho Diagnostic Systems) and anti-CR2 (IgG2a; Becton Dickinson, San Jose, CA) for CD21 and I3 (IgG2a; Coulter) for α and β complex of HLA class II. For detection of surface markers, we used anti-CD2 (Coulter), anti-CD3 (DAKO), B1 (anti-CD20; Coulter), and anti-CD94 (Coulter). Freshly isolated NK cells were stained with FITC-conjugated Leu-4 (anti-CD3 mAb; Becton Dickinson), phycoerythrin-conjugated NKH1 (anti-CD56 mAb; Coulter), and phycoerythrin-conjugated 3G8 (anti-CD16 mAb; Coulter). We also analyzed intracytoplasmic LMP1 expression with CS1–4 (mouse anti-LMP1 mAb; DAKO), using paraformaldehyde-saponin procedure as described elsewhere (37).

Western Blot Analysis. Cell lysates were prepared as previously described (38). Equal amount of total cellular protein (50 to 100 μg) prepared from each sample was separated on a discontinuous SDS-10% polyacrylamide gel, and blotted onto nitrocellulose membrane (Bio-Rad, Hercules, CA). Expression of EBNA2, LMP1, ZEBRA, and early antigen-diffuse (EA-D) was examined by using PE2, CS1-4, BZ1 (DAKO), EA-D-p52/50 (Chemi-Con, Temecula, CA), respectively. Antibody signals were enhanced using Envision polymer (DAKO) and detected with ECL Western blot detection system (Amersham International plc, Buckinghamshire, United Kingdom) according to the manufacturer's protocol.

RESULTS

Infection of Human NK Cell Lines by rEBV. We examined EBV entry into NK-92 and NKL cells using EGFP-EBV, which contains the EGFP gene in its genome. Approximately one-third of NK-92 and NKL cells were EGFP positive on confocal laser microscopy after 48 h of exposure to EGFP-EBV. Flow cytometric analysis confirmed that ~30% of both NK cell lines were positive for EGFP signal (Fig. 1). Because nonexposed and neo^r-EBV-exposed cells were negative for EGFP signal, appearance of EGFP-positive cells after EGFP-EBV exposure verified EBV infection of both NK cell lines.

Detection of EBV-Associated Gene Transcripts in rEBV-Exposed NK Cell Lines. To confirm EBV infection, we performed RT-PCR analysis of viral transcripts after 48 h of exposure to rEBV. In nonexposed NK-92 and NKL cells, we detected no EBV-associated gene transcripts, indicating that both NK cell lines are free from EBV infection. After 48 h of exposure to neo^r-EBV or EGFP-EBV, we detected *EBER1* in NK-92 and NKL cells (Fig. 2*A*). These data indicated that neo^r-EBV, as well as EGFP-EBV, infected both NK cell lines. Among six viral transcripts evaluated, we detected transcripts of Qp-initiated *EBNA1*, *BZLF1*, and *BALF2* but none of *EBNA2*, *LMP1* or *LMP2A* in rEBV-exposed NK-92 and NKL cells (Fig. 2*B*). *BZLF1*, which encodes lytic transactivator ZEBRA, and *BALF2*, which encodes a major DNA binding protein, are expressed in the lytic infection. These findings raised the possibility that latent and lytic infection coexisted in both rEBV-exposed NK cell lines. *In situ* hybridization showed that *EBERs* and *BHLFs* were transcribed in neo^r-EBV-exposed NKL cells (Fig. 3). *EBERs* are known as markers for latent infection, whereas *BHLFs*, which encode proteins belonging to the

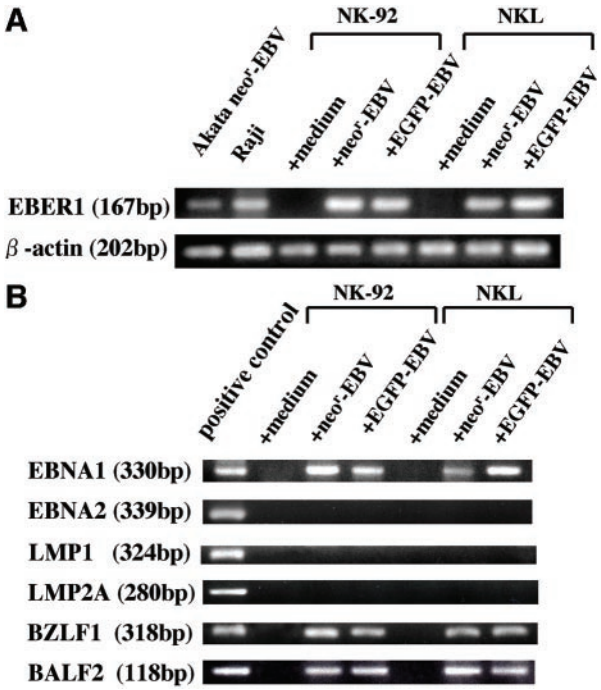

Fig. 2. Reverse transcription-PCR analysis of EBV-associated gene expression in recombinant EBV-infected natural killer (NK) cell lines. *A*, *EBER1* expression in neo^r-EBV- or EGFP-EBV-exposed NK-92 and NKL cells. *B*, nested reverse transcription-PCR analysis detected *EBNA1*, *BZLF1*, and *BALF2* but not *EBNA2*, *LMP1*, or *LMP2A* transcripts in recombinant EBV-exposed NK-92 and NKL cells. As a positive control, we used Raji in for *EBNA1*, *EBNA2*, *LMP1*, and *LMP2A* and Akata treated with 20 ng/ml 12-*O*-tetradecanoylphorbol-13-acetate (TPA) for 8 h for *BZLF1* and *BALF2*.

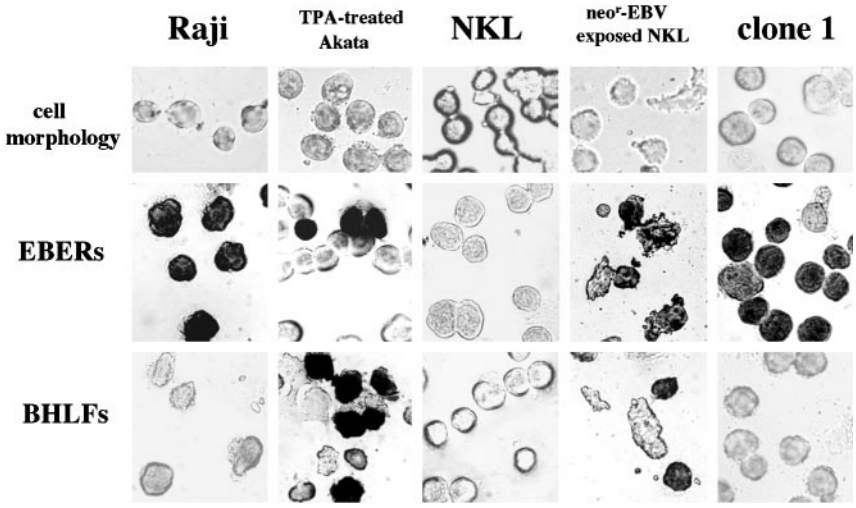

Fig. 3. RNA *in situ* hybridization of *EBERs* and *BHLFs* in neo^r-EBV-exposed NKL and established clone 1. We used Raji and 12-*O*-tetradecanoylphorbol-13-acetate (TPA)-treated Akata as positive controls for *EBERs* and *BHLFs*, respectively. After 48 h of exposure to neo^r-EBV, we detected both *EBERs* and *BHLFs* signals in NKL cells. However, only *EBERs*' signal was detected in clone 1.

subgroup of EA-D, are transcribed in the lytic infection. Highly deformed bizarre cells tended to be positive for *EBERs*' signals (Fig. 3). On the contrary, *BHLFs* were mainly transcribed in round-shaped cells (Fig. 3). These data suggest that latent and lytic phase population coexisted in neo^r-EBV-exposed NKL cells. We observed essentially the same tendency in neo^r-EBV-exposed NK-92 cells (data not shown). These results confirmed that rEBV infects NK-92 and NKL cells.

EGFP-Positive NK Cell Lines Entered Apoptotic Process. As shown in Fig. 1, we found that a considerable part of EGFP-positive NK cell lines showed a bizarre shape. Cell deformation was also observed in neo^r-EBV-exposed NK cell lines. We, then, examined whether EBV infection causes cell death in the host cells. EGFP-EBV-exposed NK cell lines were evaluated by PI rejection and annexin V-binding assays. After 48 h of exposure, no annexin V or PI signal was detected in NK-92 and NKL cells. By 72 h, however, most of EGFP-positive NK cell lines were stained with annexin V, although they remained negative for PI signal (Fig. 4). These data indicate that most of NK-92 and NKL cells entered early phase of apoptosis by 72 h after EBV-EBV infection.

NK Cell Lines Lacked CD21 but Expressed HLA Class II. EBV is known to engage CD21 in the initial attachment to target cells. We examined CD21 expression on the surface of NK-92 and NKL cells by indirect immunofluorescence and flow cytometry. We used two mAbs, OKB7 and anti-CR2, which recognizes the short consensus repeat 1-2 and the short consensus repeat 3-4 of the CD21 molecule, respectively. As shown in Fig. 5*A*, both antibodies failed to react with NK-92 or NKL cells, indicating the lack of the CD21 expression in both NK cell lines. RT-PCR analysis, which amplifies the short consensus repeat 2-3 site of the CD21 molecule, confirmed that these cell lines lack the CD21 transcripts (Fig. 5*B*). We next examined the expression of HLA class II, which acts as a coreceptor in EBV infection. Flow cytometric analysis clearly detected α and β chain complex of HLA class II on the cell surface of NK-92 and NKL (Fig. 5*A*). These findings show that both NK cell lines lack the main EBV receptor CD21 but express HLA class II β chain, which bind to gp85-gp25-gp42 complex.

Infection of PB-NK Cells by rEBV. Because NK-92 and NKL were proved to be target cells of EBV, we next evaluated whether this event was applicable to the normal PB-NK cells. We purified PB-NK cells from normal peripheral blood mononuclear cells using immunomagnet beads by the negative-selection method. Flow cytometric analysis showed that ~98% of the isolated cells were $CD3^-CD16^+$ or $CD3^-CD56^+$ (Fig. 6*A*). The purified cells were exposed to rEBV in the same way as the two NK cell lines. At least 98% of the medium-exposed PB-NK population remained $CD3^-CD16^+$ or $CD3^-CD56^+$ for 48 h (Fig. 6*A*). Confocal microscopy detected EGFP signal in EGFP-EBV-exposed PB-NK cells after 48 h of incubation. Flow cytometric analysis confirmed that >45% of PB-NK cells were EGFP positive (Fig. 6*B*). EGFP signal was detected in ~74 and 90% of EGFP-EBV-exposed PB-NK cells from two other volunteers (Fig. 6*C*). In comparison to the nonexposed PB-NK cells, rEBV-exposed ones became larger in size. Giant cell formation was obvious in addition to cell deformation in PB-NK cells after rEBV infection.

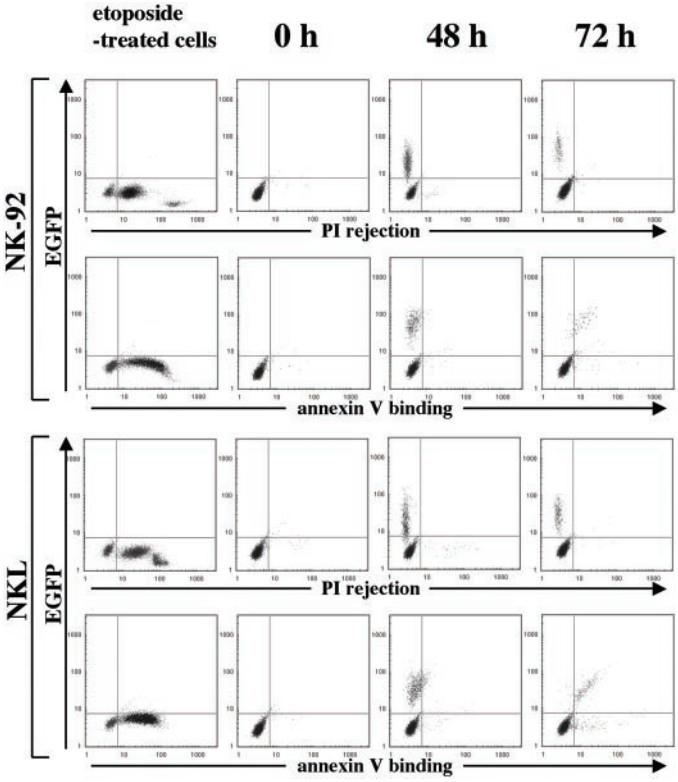

Fig. 4. Propidium iodide (PI) rejection and annexin V binding assays in EGFP-EBV-exposed natural killer (NK) cell lines. NK-92 (*top two columns*) and NKL (*bottom two columns*) were evaluated for cell death after exposure to EGFP-EBV. At 48 h, no PI or annexin V signal was detected in both NK cell lines. At 72 h, EGFP-positive NK-92 and NKL cells were positive for annexin V but not for PI. As a positive control, we treated both NK cell lines treated with 1 mM etoposide for 12 h as a positive control.

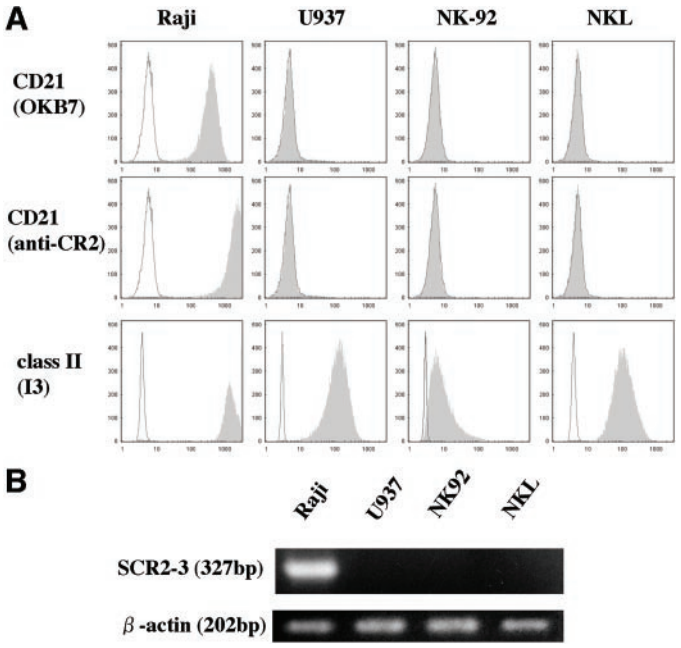

Fig. 5. HLA class II but not CD21 expression levels in NK-92 and NKL cells. *A*, flow cytometric analysis detected HLA class II but not CD21 in NK92 and NKL cells (solid histogram). Open histogram shows the result obtained with a control monoclonal antibody. *B*, reverse transcription-PCR analysis detected no CD21 transcripts in NK-92 and NKL cells. In *A* and *B*, Raji and U937 were used as positive and negative controls, respectively.

Establishment of EBV-Carrying NKL Cells. After G418 selection, we obtained two G418-resistant clones containing EBV from neo^r-EBV-exposed NKL cells. Although we tried to establish EBV-carrying NK-92 and PB-NK cells, most of rEBV-exposed cells died within 1 week after the start of G418 selection. In comparison to original cells, the two established NKL clones tended to have nuclear deformation such as indented nuclei or micronuclei (Fig. 7*A*). Surface marker expressions such as CD2, CD3, CD20, and CD94 were essentially the same among original and two obtained NKL clones (Fig. 7*B*).

RT-PCR analysis detected transcripts of major lytic genes, *BZLF1* and *BALF2* in addition to *EBER1* and Qp-initiated *EBNA1* in both clones (Fig. 8, *A* and *B*). The pattern was the same as that observed at 48 h of EBV exposure. However, Western blot analysis failed to detect ZEBRA and EA-D in these clones (Fig. 9*B*). This discordance is probably because of too high sensitivity of nested PCR analysis. *In situ* hybridization also detected *EBERs* but not *BHLFs* in clone 1, which supported the results of Western blot analysis (Fig. 3). These findings indicated that latent EBV infection but not lytic infection was maintained in these clones.

Although *LMP1* and *LMP2A* transcripts were undetectable during the early phase of EBV infection, we detected them in clone 1 by RT-PCR analysis (Fig. 8*B*). Western blotting and flow cytometric analysis confirmed LMP1 expression in clone 1 (Fig. 9, *A* and *B*). Therefore, LMP1 expression should be restricted only after establishment of EBV-carrying NKL clone. LMP1 from clone 1 was apparently $<$60 kDa on Western blot analysis (Fig. 9*B*). The band appeared to be the truncated form, which is usually observed at the early phase of EBV infection. *EBNA2* was never detected even by RT-PCR analysis during the entire process of EBV infection. Analysis of various clinical samples including nasal-type NK cell lymphomas has shown the LMP1 expression despite the lack of EBNA2. Here, we demonstrated the same expression pattern of EBV-associated genes *in vitro*.

DISCUSSION

Considerable part of NK cell neoplasms possess EBV genome. However, there has been no direct evidence that EBV infects human NK cells. In this study, we used EGFP-EBV to monitor the entry of EBV into human NK cells. Because EGFP signal is generated only after the entry of EGFP-EBV into the target cells, we confirmed EGFP-EBV infection of two NK cell lines and PB-NK cells.

Although it remains unclear whether naive PB-NK cells express the CD21 molecule, our present results showed the lack of CD21 expression in NK-92 and NKL cells. Recent studies have also shown the infection of several human CD21-negative cell lines by EBV (21–23, 25). Janz *et al.* (24) showed that rEBV lacking gp350/220, a ligand for CD21, infects Raji cells. Although the role of the CD21-mediated pathway during the primary NK cell infection by EBV is controversial, our results support the presence of an unknown virus-cell interaction distinct from the CD21-mediated pathway. HLA class II β

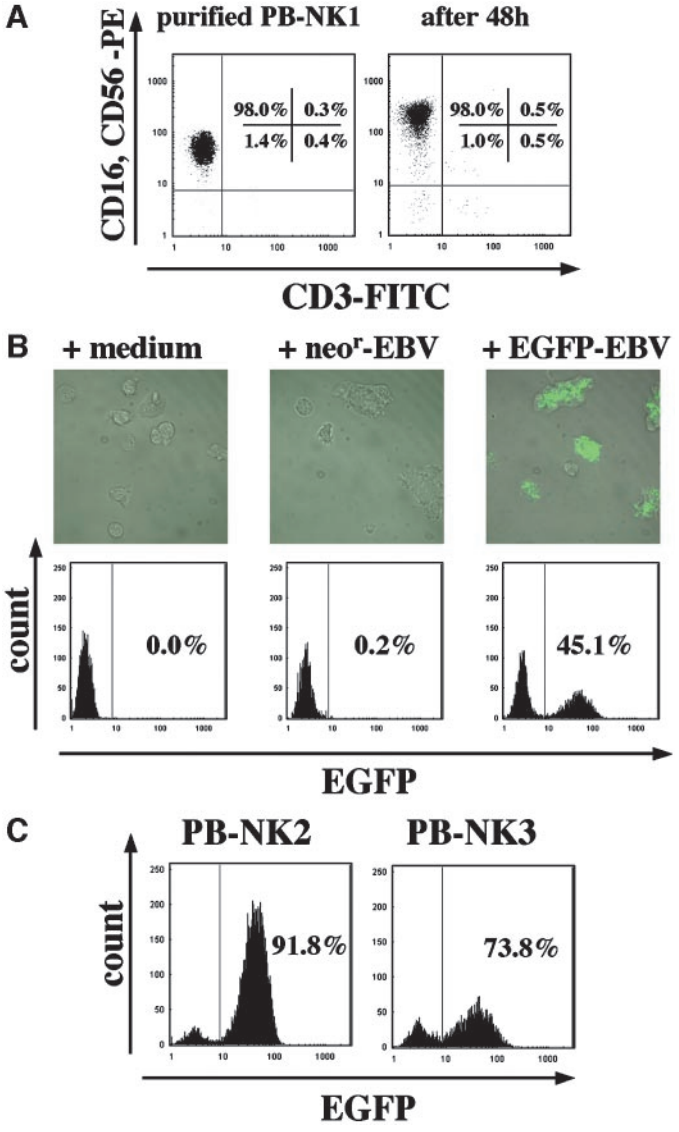

Fig. 6. EBV infects normal peripheral blood natural killer (PB-NK) cells. PB-NK cells purified from normal donors were exposed to medium, neo^r-EBV, or EGFP-EBV. *A*, approximately 98% of the purified cells were $CD3^-CD16^+$ or $CD3^-CD56^+$ even after 48 h of incubation. *B*, confocal laser microscopy (*top column*) and flow cytometry (*bottom column*) detected enhanced green fluorescent protein (EGFP) signal only in EGFP-EBV-exposed PB-NK cells. *C*, more than 70% of PB-NK cells from other two volunteers were also positive for EGFP signal.

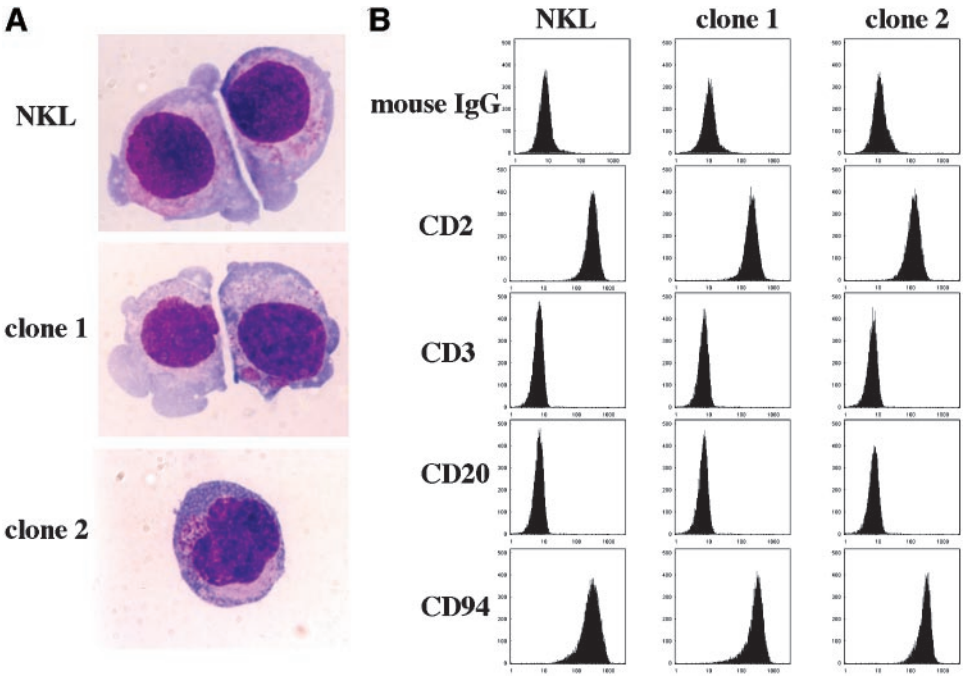

Fig. 7. Characterization of two EBV-carrying NKL clones. Two G418-resistent clones were obtained from neo^r-EBV-exposed NKL cells. *A*, Wright-Giemsa staining of two established clones (clone 1 and clone 2) and original NKL cells (×1000). *B*, expression patterns of CD2, CD3, CD20, and CD94 were essentially the same among clone 1, clone 2, and original cells.

chains are believed to be important for EBV internalization in HLA class II-positive cells (18, 19, 39). Viral glycoproteins, gp42 and gp85, are known to play an important role in EBV internalization into HLA class II-positive cells (21, 39). We detected expression of HLA class II on the cell surface of both NK cell lines. Activated PB-NK cells are known to express HLA class II. Therefore, after binding to EBV through a distinct molecule from CD21, both NK cell lines and PB-NK cells may fuse with EBV through the association between the ternary complex and the HLA class II β chain.

Type I and II latency patterns are recognized in EBV-associated NK cell malignancies (13, 14). In the early phase of EBV infection, even RT-PCR analysis detected only *EBER1* and Qp-initiated *EBNA1* transcripts among the latent genes examined in rEBV-exposed NK-92 and NKL cells. This expression pattern corresponds to type I latency.

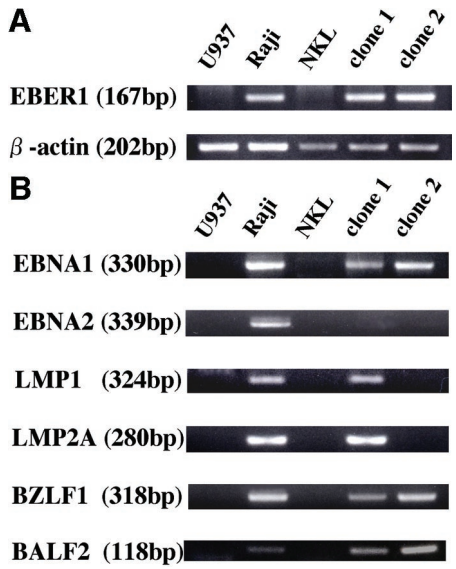

Fig. 8. Reverse transcription-PCR analysis of EBV-associated genes in EBV-carrying NKL clones. *A*, *EBER1* was expressed in EBV-carrying NKL clones. *B*, nested PCR analysis detected not only *EBNA1* but also *BZLF1* and *BALF2* in both clones. *LMP1* and *LMP2A* transcripts were positive only in clone 1.

However, RT-PCR analysis detected *LMP1* but not *EBNA2* transcript after establishment of NKL-derived clone 1, which corresponds to type II latency. Western blotting and flow cytometric analysis confirmed LMP1 expression in clone 1. Therefore, expression of LMP1 in this clone should be independent of EBNA2. A similar expression pattern of EBV-associated genes was reported in EBV-infected peripheral blood T cells. In the early phase of infection, EBV-infected peripheral blood T cell was reported to lack LMP1 expression (40). However, established EBV-carrying peripheral blood T-cell clones were shown to express LMP1 (41, 42). The temporal profile of latent gene expression pattern during EBV infection in NK cells may be similar to that in peripheral blood T cells.

Although a truncated form of LMP1 is known to appear early after EBV infection or at the lytic phase in B cells (43, 44), we detected only the truncated form at the latent phase in clone 1. Detection of shorter sizes of LMP1 was also reported in clinical samples from patients of nasopharyngeal carcinoma (45). We suppose that some differences at the transcription and translation levels in host cells may lead to the generation of aberrant sizes of LMP1.

In the early phase of infection, we detected *BZLF1* and *BALF2* transcripts in addition to latent gene expression in rEBV-exposed NK-92 and NKL cells by RT-PCR. Because the results suggested the presence of cells in latent and lytic phases, we additionally evaluated the expression of latent and lytic infection genes by *in situ* hybridization. In NKL, *in situ* hybridization showed that lytic and latent phase populations coexisted in EBV-exposed cells after 48 h of exposure. Although RT-PCR analysis detected *BZLF1* and *BALF2* transcripts even in two established NKL clones, Western blot analysis failed to detect ZEBRA and EA-D proteins in them. *In situ* hybridization supported this result. Although we cannot fully explain the reason for detection of *BZLF1* transcripts, we suppose that expression of *BZLF1* may not be so strictly shut-off that nested RT-PCR analysis detected a tiny amount of the transcripts. Therefore, nested RT-PCR analysis alone should not warrant the biologically relevant levels of EBV-associated gene expression. Indeed, nonproducer cell line Raji was reported to express *BZLF1* by RT-PCR technique (33).

We found that some of rEBV-exposed NK cell lines were highly deformed into a bizarre shape. This phenomenon occurred in consid-

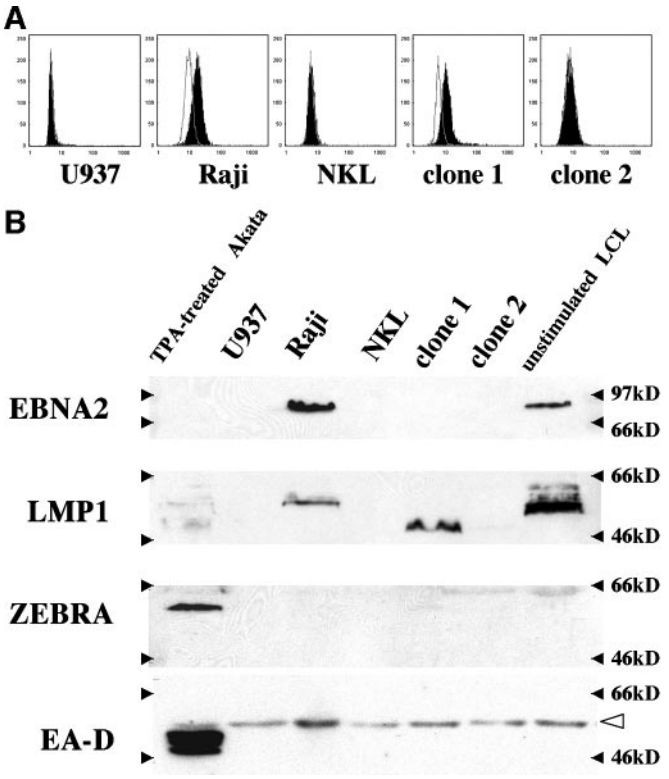

Fig. 9. Clone 1 expresses LMP1. *A*, flow cytometric analysis showed LMP1 expression only in clone 1. Raji and U937 were used as positive and negative controls, respectively. *B*, clone 1 expresses LMP1 but not EBNA2 in Western blot analysis. Lytic infection markers, ZEBRA and EA-D, were not detected in Raji and the two clones. In EA-D evaluation, nonspecific bands (*arrowhead*) at upper site of 52 kDa EA-D warrants almost equal amount of protein loading. 12-*O*-Tetradecanoylphorbol-13-acetate (TPA)-treated Akata was used as a positive control for expression of ZEBRA and EA-D.

erable part of EGFP-positive cells. *In situ* hybridization showed that NKL cells with abnormal cell shape were usually positive for *EBERs*' signal, which suggests that dominant part of EGFP-positive cells showed cell deformation and may enter latent phase of infection. In case of PB-NK cells, cell enlargement in addition to bizarre cell shape was observed after EBV infection. Primary EBV infection of B and T cells was reported to cause Reed-Sternberg cell-like giant cell formation (46). Furthermore, *in situ* hybridization demonstrated that giant cells were in latent phase, whereas cells in lytic phase showed a more rounded shape (46). This study is in good accordance with the present results. EBV-induced giant cells have been believed to be syncytia, which result from the fusion of infected cells (47). However, Secchiero *et al.* (48) suggests another possibility of giant cell formation in human herpesvirus-7-infected T cells, *i.e.*, polyploidization with abortive cytokinesis. We suppose that EBV may cause deformation of the infected cell shape through alternation in cytoskeletal components and cell cycle disturbance, including polyploidization. Furthermore, our results showed that most of EGFP-EBV-infected NK-92 and NKL cells enter apoptosis, which explains difficulties in establishing EBV-carrying NK cells *in vitro*. However, EGFP-EBV enables us to show the EBV infection of human NK cells at an earlier phase than the excursion of apoptosis.

This is the first study clearly showing that EBV infects human NK cells. We observed essentially the same expression pattern of EBV-associated genes in EBV-infected NK-cell lines *in vitro* as that reported in clinical samples. Although additional studies are required to confirm the critical role of EBV in the development of NK-cell neoplasms, this work may be the first step to elucidate this point.

ACKNOWLEDGMENTS

We thank Dr. Jiang-Hong Gong (University of British Columbia, Vancouver, Canada) and Dr. Michael J. Robertson (Harvard Medical School, Boston, MA) for providing NK-92 and NKL, respectively. We also thank Ayako Okamoto and Keiko Hayashi for technical assistance.

REFERENCES

1. Rickinson AB, Kieff E. Epstein-Barr virus. *In:* Knipe, DM, Howley, PM, editors. Fields virology, 4th ed., Vol. 2. Philadelphia: Lippincott Williams & Wilkins; 2001. p. 2575–628.
2. Cohen JI. Epstein-Barr virus infection. N Engl J Med 2000; 343:481–92.
3. Kawa-Ha K, Ishihara S, Ninomiya T, et al. CD3-negative lymphoproliferative disease of granular lymphocytes containing Epstein-Barr viral DNA. J Clin Investig 1989; 84:51–5.
4. Hart DNJ, Baker BW, Inglis MJ, et al. Epstein-Barr viral DNA in acute large granular lymphocyte (natural killer) leukemic cells. Blood 1992;79:2116–23.
5. Kaneko T, Fukuda J, Yoshihara T, et al. Nasal natural killer (NK) cell lymphoma: report of a case with activated NK cells containing Epstein-Barr virus and expressing CD21 antigen, and comparative studies of their phenotype and cytotoxicity with normal NK cells. Br J Haematol 1995;91:355–61.
6. Jaffe ES, Chan JKC, Su IJ, et al. Report of the workshop on nasal and related extranodal angiocentric T/natural killer cell lymphomas: definitions, differential diagnosis, and epidemiology. Am J Surg Pathol 1996;20:103–11.
7. Jaffe, ES, Harris, NL, Vardiman JW, editors. Mature T-cell and NK-cell neoplasms. In: World Health Organization classification of tumours. Pathology and genetics of tumours of haematopoietic and lymphoid tissues. Lyon: IARC Press, 2001. p. 189–236.
8. Nakamura S, Katoh E, Koshikawa T, et al. Clinicopathologic study of nasal T/NK-cell lymphoma among the Japanese. Pathol Int 1997;47:38–53.
9. Imamura N, Kusunoki Y, Kawa-Ha K, et al. Aggressive natural killer cell leukemia/lymphoma: report of four cases and review of the literature. Br J Haematol 1990;75: 49–59.
10. Tefferi A, Li CY, Witzig TE, et al. Chronic natural killer cell lymphocytosis: a descriptive clinical study. Blood 1994;84:2721–5.
11. Oshimi K. Leukemia and lymphoma of natural killer lineage cells. Int J Hematol 2003;78:18–23.
12. Kieff E, Rickinson AB. Epstein-Barr virus and its replication. In: Knipe DM, Howley PM, editors. Fields virology, 4th ed., Vol. 2. Philadelphia: Lippincott Williams & Wilkins, 2001. p. 2511–74.
13. Chiang AKS, Tao Q, Srivastava G, Ho FCS. Nasal NK- and T-cell lymphomas share the same type of Epstein-Barr virus latency as nasopharyngeal carcinoma and Hodgkin's disease. Int J Cancer 1996;68:285–90.
14. Mizuno S, Akashi K, Ohshima K, Iwasaki H, Miyamoto T, Uchida N, Shibuya T, Harada M, Kikuchi M, Niho Y. Interferon-γ prevents apoptosis in Epstein-Barr virus infected natural killer cell leukemia in an autocrine fashion. Blood 1999;93:3494–504.
15. Tokura Y, Ishihara S, Tagawa S, Seo N, Oshima K, Takigawa M. Hypersensitivity to mosquito bites as the primary clinical manifestation of a juvenile type of Epstein-Barr virus-associated natural killer cell leukemia/lymphoma. J Am Acad Dermatol 2001; 45:569–78.
16. Kimura H, Morishima T, Kanegane H, et al. Prognostic factors for chronic active Epstein-Barr virus infection. J Infect Dis 2003;187:527–33.
17. Tanner J, Weis J, Fearon D, Whang Y, Kieff E. Epstein-Barr virus gp350/220 binding to the B lymphocyte C3d receptor mediates adsorption, capping, and endocytosis. Cell 1987;50:203–13.
18. Speck P, Haan KM, Longnecker R. Epstein-Barr virus entry into cells. Virology 2000;277:1–5.
19. Li Q, Spriggs M, Kovats S, et al. Epstein-Barr virus uses HLA class II as a cofactor for infection of B lymphocytes. J Virol 1997;71:4657–62.
20. Haan KM, Kwok WW, Longnecker Rm Speck P. Epstein-Barr virus entry utilizing HLA-DP or HLA-DQ as a coreceptor. J Virol 2000;74:2451–4.
21. Molesworth SJ, Lake CM, Borza CM, Turk SM, Hutt-Fletcher LM. Epstein-Barr virus gH is essential for penetration of B cells but also plays a role in attachment of virus to epithelial cells. J Virol 2000;74:6324–32.
22. Yoshiyama H, Imai S, Shimizu N, Takada K. Epstein-Barr virus infection of human gastric carcinoma cells: implication of the existence of a new virus receptor different from CD21. J Virol 1997;71:5688–91.
23. Imai S, Nishikawa J, Takada K. Cell-to-cell contact as an efficient mode of Epstein-Barr virus infection of diverse human epithelial cells. J Virol 1998;72:4371–8.
24. Janz A, Oezel M, Krzeder C, et al. Infectious Epstein-Barr virus lacking major glycoprotein BLLF1 (gp350/220) demonstrates the existence of additional viral ligands. J Virol 2000;74:10142–52.
25. Maruo S, Yang L, Takada K. Roles of Epstein-Barr virus glycoproteins gp350 and gp25 in the infection of human epithelial cells. J Gen Virol 2001;82:2373–83.
26. Speck P, Longnecker R. Epstein-Barr virus (EBV) infection visualized by EGFP expression demonstrates dependence on known mediators of EBV entry. Arch Virol 1999;144:1123–37.
27. Yoshiyama H, Shimizu N, Takada K. Persistent Epstein-Barr virus infection in a human T-cell line: unique program of latent virus expression. EMBO J 1995;14: 3706–11.
28. Gong JH, Maki G, Klingemann HG. Characterization of a human cell line (NK-92) with phenotypical and functional characteristics of activated natural killer cells. Leukemia (Baltimore) 1994;8:652–8.

29. Robertson MJ, Cochran KJ, Cameron C, Le JM, Tantravahi R, Ritz J Characterization of a cell line, NKL, derived from an aggressive human natural killer cell leukemia. Exp Hematol 1996;24:406–15.
30. Takada K, Horinouchi K, Ono Y, Aya T, Osato T, Takahashi M, Hayasaka S. An Epstein-Barr virus-producer line Akata: establishment of the cell line and analysis of viral DNA. Virus Genes 1991;5:147–56.
31. Takada K. Cross-linking of cell surface immunoglobulins induces Epstein-Barr virus in Burkitt lymphoma lines. Int J Cancer 1984;33:445–9.
32. Sugiura M, Imai S, Tokunaga M, Koizumi S, Uchizawa M, Okamoto K, Osato T. Transcriptional analysis of Epstein-Barr virus gene expression in EBV-positive gastric carcinoma: unique viral latency in the tumour cells. Br J Cancer 1996;74:625–31.
33. Tao Q, Robertson KD, Manns A, Hildesheim A, Ambinder RF. Epstein-Barr virus (EBV) in endemic Burkitt lymphoma: molecular analysis of primary tumor tissue. Blood 1998;91:1373–81.
34. Kitagawa N, Goto M, Kurozumi K, et al. Epstein-Barr virus-encoded poly (A)-RNA supports Burkitt lymphoma growth through interleukin-10 induction. EMBO J 2000; 19:6742–50.
35. Prang NS, Hornef MW, Jager M, Wagner HJ, Wolf H, Schwarzmann FM. Lytic replication of viral gene expression in B lymphocytes during infectious mononucleosis and in the normal carrier state. Blood 1997;89:1665–77.
36. Busson P, McCoy R, Sadler R, Gilligan K, Tursz T, Raab-Traub N. Consistent transcription of the Epstein-Barr virus LMP2 gene in nasopharyngeal carcinoma. J Virol 1992;66:3257–62.
37. Sander B, Andersson J, Andersson U. Assessment of cytokines by immunofluorescence and the paraformaldehyde-saponin procedure. Immunol Rev 1991;119:65–93.
38. Sugimoto K, Yamada K, Egashira M, et al. Temporal and spatial distribution of DNA topoisomerase II alters during proliferation, differentiation, and apoptosis in HL-60 cells. Blood 1998;91:1407–17.
39. Borza CM, Hutt-Fletcher LM. Alternate replication in B cells switches tropism of Epstein-Barr virus. Nat Med 2002;8:594–9.
40. Guan M, Zhang RD, Wu B, Henderson EE. Infection of primary $CD4^+$ and $CD8^+$ T lymphocytes by Epstein-Barr virus enhances human immunodeficiency virus expression. J Virol 1996;70:7341–6.
41. Imai S, Sugiura M, Oikawa O, et al. Epstein-Barr virus (EBV)-carrying and -expressing T-cell lines established from severe chronic active EBV infection. Blood 1996; 87:1446–57.
42. Groux H, Cottrez F, Montpellier C, et al. Isolation and characterization of transformed human T-cell lines infected by Epstein-Barr virus. Blood 1997;89:4521–30.
43. Erickson KD, Martin JM. Early detection of the lytic LMP-1 protein in EBV-infected B-cells suggests its presence in the virion. Virology 1997;234:1–13.
44. Rowe M, Evans HS, Young LS, Hennessy K, Kieff E Rickinson AB. Monoclonal antibodies to the latent membrane protein of Epstein-Barr virus reveal heterogeneity of the protein and inducible expression in virus-transformed cells. J Gen Virol 1987;68:1575–86.
45. Hu L, Troyanovsky B, Zhang X, Trivedi P, Ernberg I, Klein G. Differences in the immunogenicity of latent membrane protein 1 (LMP1) encoded by Epstein-Barr virus genomes derived from LMP1-positive and -negative nasopharyngeal carcinoma. Cancer Res 2000;60:5589–93.
46. Anagnostopoulos I, Hummel M, Kreschel C, Stein H. Morphology, immunophenotype, and distribution of latently and/or productively Epstein-Barr virus-infected cells in acute infectious mononucleosis: Implications for the interindividual infection route of Epstein-Barr virus. Blood 1995;85:744–50.
47. Bayliss GJ, Wolf H. An Epstein-Barr virus early protein induces cell fusion. Proc Natl Acad USA 1981;78:7162–5.
48. Secchiero P, Bertolaso L, Casareto L, et al. Human herpesvirus 7 infection induces profound cell cycle perturbations coupled to disregulation of cdc2 and cyclin B and polyploidization of $CD4^+$ T cells. Blood 1998;92:1685–96.